Journal of Materials Chemistry

Cite this: *J. Mater. Chem.*, 2011, **21**, 13470

www.rsc.org/materials

PAPER

A ratiometric fluorescent pH probe based on aggregation-induced emission enhancement and its application in live-cell imaging†

Panshu Song,[a] Xiaotong Chen,[a] Yu Xiang,[b] Lei Huang,[c] Zhaojuan Zhou,[a] Ruirui Wei[a] and Aijun Tong*[a]

Received 12th May 2011, Accepted 20th June 2011
DOI: 10.1039/c1jm12098k

A ratiometric fluorescent pH probe, 4-carboxylaniline-5-chlorosalicylaldehyde Schiff base (**1**) was synthesized *via* a facile reaction and used for pH sensing in live cells. While exhibiting weak fluorescence when dispersed in solution, **1** displayed aggregation-induced emission enhancement (AIEE) characteristics in its aggregate/solid state, as a result of the restriction of free intramolecular rotation of a C–N bond and the non-planar configuration in the aggregate/solid state. The integration of hydroxyl and carboxyl groups provided **1** with a ratiometric fluorescent response to pH based on AIEE and the pH-dependent spectral characteristics of compound **1**, with proton dissociation constants pK_{a1} and pK_{a2} of 4.8 ± 0.1 and 7.4 ± 0.1, respectively. The probe exhibited a significant fluorescence color change from orange to green with an intensity ratio ($I_{516\ nm}/I_{559\ nm}$) enhanced when the pH increased from 5.0 to 7.0 in aqueous solution. Confocal fluorescence imaging of intracellular pH through ratiometric response was successfully achieved in live HepG2 cells. The results demonstrate that probe **1** is a good candidate for monitoring pH fluctuations in live cells with good selectivity, stability, and excellent membrane permeability.

Introduction

The development of optical sensors for intracellular pH monitoring has attracted great attention since fluctuations in intracellular pH play an essential role in many cellular processes such as cell growth, enzyme activity and ion transport,[1] and variations in intracellular pH is a common phenotype of cancer cells.[2] In particular, fluorescent pH probes with ratiometric properties are highly preferred for pH monitoring in complex samples because of their visible fluorescence color change and better resistance to variations of sensor concentration and external environment.[3] By combining the use of a fluorescent pH probe and an appropriate imaging instrument, fluorescent imaging of pH provides a promising method for studying pH fluctuations in live cells. However, only a limited number of ratiometric pH probes have been reported to be practical for intracellular fluorescent imaging, and the synthetic procedures for these compounds are often complicated.[4]

In recent years, fluorophores displaying aggregation-induced emission enhancement (AIEE) have provided a powerful platform for the development of novel chemical and biological sensors.[5] It is well known that many organic fluorescent materials exhibit very strong fluorescence in dilute solution, however their emission intensities dramatically decrease with increasing concentrations and formation of aggregates. This aggregation-caused quenching (ACQ) effect mainly results from strong intermolecular π–π stacking interactions and non-radiative decay.[6] In contrast, AIEE fluorophores, as first reported by Tang and Zhu *et al.* in 2001,[7] are weakly fluorescent when dispersed in solution, but exhibit intense fluorescence in an aggregate or solid state.[8] The restriction of the intramolecular rotation (RIR) process and the non-planar configuration in their aggregate state which experiences little π–π stacking interactions are regarded as the main causes for the AIEE effect.[9] Hence, a design principle of AIEE molecules is to have two or more conjugated/aromatic moieties connected by rotatable single bond(s), which result in nonradiative decay in the solution state, but an enhanced emission in the aggregate state when rotation is restricted.[10] On the basis of this principle, a series of salicylaldehyde azine derivatives were previously studied in our group, which exhibited AIEE characteristics by restriction of intramolecular rotation of a N–N single bond when changed from solution to aggregate state.[11] Although AIEE compounds bearing pH sensitive groups have been shown to demonstrate a pH-dependent fluorescence response, there is still no such dye reported with a ratiometric fluorescence response in near-neutral pH ranges.[12]

[a]*Department of Chemistry, Tsinghua University, Beijing, 100084, PR China. E-mail: tongaj@mail.tsinghua.edu.cn; Fax: +86-10-62787682; Tel: +86-10-62787682*
[b]*Department of Chemistry, University of Illinois at Urbana-Champaign, Urbana, IL, 61801, USA*
[c]*Center of Biomedical Analysis, Tsinghua University, Beijing, 100084, PR China*

† Electronic supplementary information (ESI) available: Scheme S1 and Fig. S1–S8. CCDC reference number 780526. For ESI and crystallographic data in CIF or other electronic format see DOI: 10.1039/c1jm12098k

In this study, an AIEE-active fluorophore, 4-carboxylaniline-5-chlorosalicylaldehyde Schiff base (**1**), was facilely synthesized for sensing pH variations in aqueous solution and in live cells. This compound showed a ratiometric fluorescent response over the pH range 5.0 to 7.0 with a fluorescence color change from orange to green, by the switching of its aggregate and solution state fluorescence (Scheme 1). Demonstrating good stability, membrane permeability, and selectivity over metal ions, compound **1** was successfully applied to intracellular pH measurement in human hepatocellular liver carcinoma cell line (HepG2 cells) by confocal microscopy.

Results and discussion

Single crystal structure

Single crystal of compound **1** was grown from ethanol solution and characterized by X-ray crystallography. As shown in Fig. 1, the crystal structure of **1** contained an intramolecular hydrogen bond in the salicylaldimine moiety, which ensured two conjugated/aromatic moieties connected by a rotatable single bond (C8–N1), indicating that **1** had the potential of aggregation-induced emission enhancement (AIEE) feature resulting from the restriction of free intramolecular rotation in its aggregate/solid state.[11,13] In addition, it was found that the carboxyl and two phenyl groups of the molecule are diorientational due to the rotation of a C11–C14 single bond which gives a statistical mirror symmetry to meet the requirement of the *C*2/*m* space group. A dihedral angle of 49.9° for the [C10-C11-C12] and [O2-C14-O3] was observed, owing to the propeller-like structure of the carboxyl groups. Furthermore, the inter-plane distances between adjacent molecules were as long as 4.32 Å (see Fig. S3. †) due to the non-planar configuration of compound **1**, which hindered any closer packing. In this case, the concentration-quenching effect caused by strong intermolecular π–π stacking interactions might be weakened in such structures.[14]

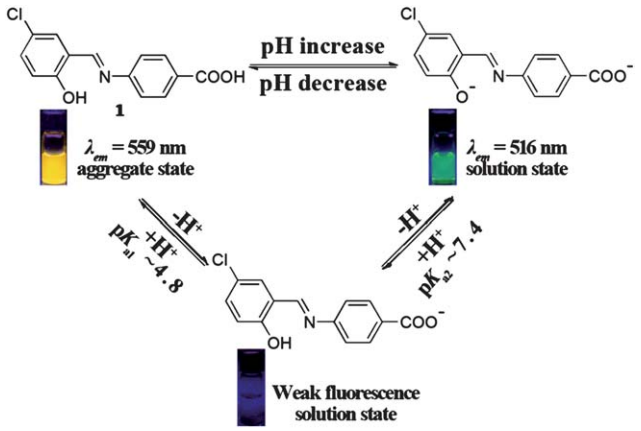

Scheme 1 Proposed deprotonation processes of compound **1**.

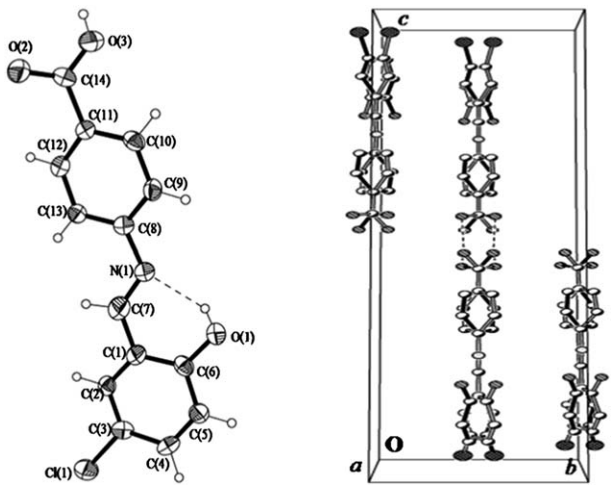

Fig. 1 Crystal structure of compound **1**. Left: ORTEP drawing with 35% probability ellipsoids. Right: A packing view along the *a* direction; the open bonds showed one orientation of the phenyl and carboxyl groups, and the solid bonds showed the other orientation.

AIEE characteristics

Compound **1** was soluble in some common organic solvents, such as ethanol, chloroform, THF, and DMF. However, water was a poor solvent. Herein, the AIEE feature of **1** was investigated in ethanol/water (from 9 : 1 to 1 : 9, v/v) buffered with 50 mM sodium phosphate at pH 4.42 (Fig. 2). In a good solvent

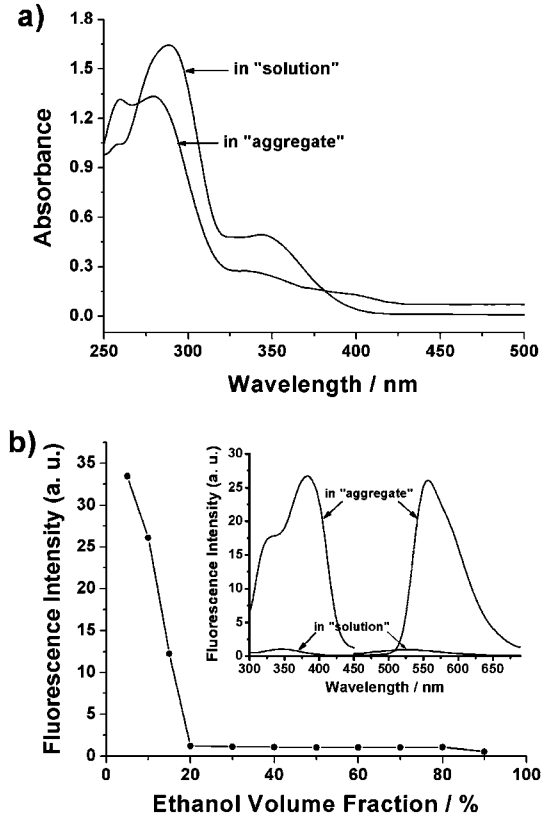

Fig. 2 (a) Absorption spectra of **1** (90 μM) in "solution" (ethanol/water, 9 : 1, v/v) and "aggregate" (ethanol/water, 1 : 9, v/v) states, containing 50 mM sodium phosphate at pH 4.42; (b) effect of ethanol volume fraction on the AIEE fluorescence intensity measured at 559 nm (peaks in emission spectra). Insert: fluorescence excitation/emission spectra of **1** in "solution" and "aggregate" states. Excitation was performed at 381 nm.

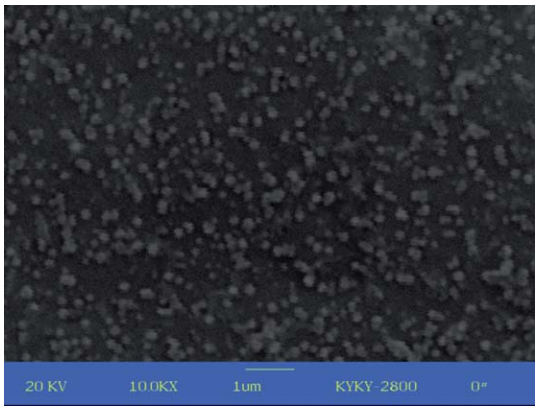

Fig. 3 SEM image for solids of **1** obtained from a suspension in 1 : 9 ethanol/water (v/v), buffered by 50 mM sodium phosphate at pH 4.42.

of 9 : 1 ethanol/water, **1** was well dispersed in its "solution" state with a structured absorption spectra, and displayed weak fluorescence emission ($\Phi_F = 0.001$). However, when **1** was dispersed in 1 : 9 ethanol/water, a leveling-off in the visible region of its absorption spectra (commonly observed in nanoaggregate suspensions[15]) strongly suggested the formation of a poorly-soluble "aggregate" state, and an intense fluorescence enhancement was observed ($\Phi_F = 0.12$) with a similar emission wavelength as observed in its solid state (powder and crystal) fluorescence spectra (see Fig. S4 †). The blue-shift observed in the absorption spectrum and the bathochromic shift in its emission spectrum were attributed to the formation of an *H*-aggregate in the aggregate/solid state of **1** with respect to its isolated chromophore, which was supported by the face-to-face arrangement in its single crystal structure.[16] The AIEE effect of compound **1** could be explained by the blocking of nonradiative intramolecular rotation decay of excited molecules, as well as by formation of a non-planar configuration in its aggregate/solid state which weakened the π–π stacking interaction. As illustrated in Fig. 2b, the AIEE effect of **1** occurred at 20% volume fraction of ethanol. A lower ethanol volume fraction was found to enhance the AIEE fluorescence intensity, which was well consistent with the fact that more aggregates would be formed in poorer solvents. Besides absorption and fluorescence spectra, the formation of aggregates of **1** was also directly observed using scanning electron microscopy (SEM): particle size distributions with 100–200 nm were detected when the solids of **1** were obtained from the solvent mixtures with 90% buffered water (pH 4.42) (see Fig. 3); while no particle was observed when the volume fraction of ethanol was above 20%.

pH-dependent optical properties

In buffer solution at pH 3.95, **1** (10 μM) exhibited absorption bands at 258 and 290 nm respectively (Fig. S5a. †). With pH values increased to 9.52, a new absorption band at 390 nm was observed, with absorbance enhanced in the 250–275 nm region and decreased in the 280–350 nm region through two pseudo-isosbestic points located at 276 and 353 nm.

The pH-dependent fluorescence response of **1** was also investigated. A ratiometric fluorescence pattern was clearly observed when the solution of **1** (60 μM) was excited at 353 nm. As

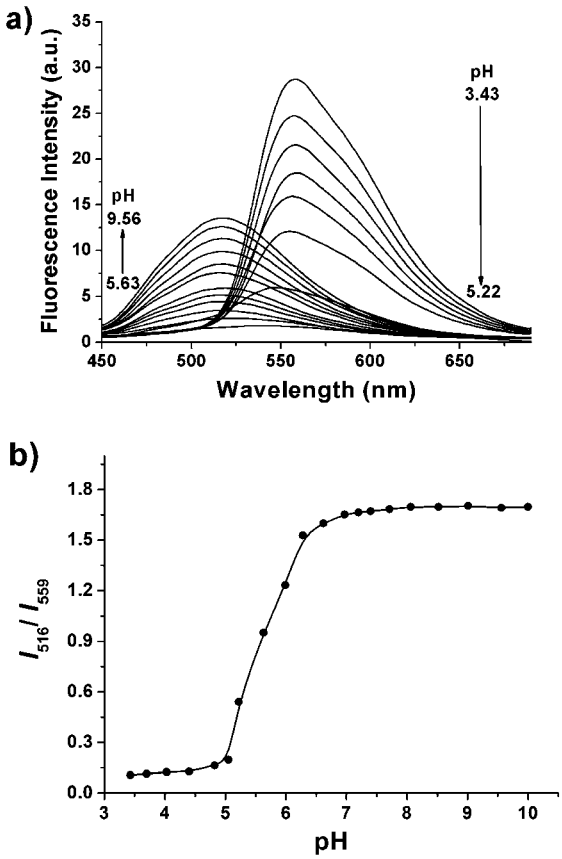

Fig. 4 (a) pH-dependence of the emission spectra of **1** (60 μM) in 50 mM phosphate buffer, with arrows indicating the change of fluorescence intensities with pH increase. From acidic to basic conditions: pH 3.43, 3.70, 4.03, 4.40, 4.82, 5.05, 5.22, 5.63, 6.00, 6.28, 6.62, 6.97, 7.20, 7.40, 7.71, 8.06, 8.52, 9.01, and 9.56; (b) ratiometric calibration curve of I_{516}/I_{559} (intensity at 516 nm *vs.* intensity at 559 nm). Excitation was performed at 353 nm.

demonstrated in Fig. 4, the neutral form of **1** tended to aggregate at acidic pH and exhibited AIEE with a fluorescence maximum at 559 nm. The AIEE effect was weakened as pH increased from 3.43 to 5.63, when the carboxyl group was deprotonated ($pK_{a1} = 4.8 \pm 0.1$, Fig. S5b.†) and the anionic form of **1** became well-dispersed in aqueous solution. As pH was further increased from 5.63 to 9.56, the hydroxyl group of compound **1** was deprotonated ($pK_{a2} = 7.4 \pm 0.1$, Fig. S5c.†), electron delocalization from the phenolate to the carbon of the imine group was enhanced due to the negative charge on the oxygen in the phenolate group. Intramolecular charge transfer (ICT) was thus enhanced as a result of the expansion of the conjugated system and the stronger electron-donating ability of the phenolate group.[17] Therefore, a new emission peak for the dianion form of **1** appeared at 516 nm in a higher pH solution. In particular, the fluorescence color changed from orange to green with an intensity ratio ($I_{516\ nm}/I_{559\ nm}$) enhancement observed over the pH range of 5.0 to 7.0, which is ideal for accurate near-neutral pH measurements.

Testifying the stability and selectivity

The photostability of probe **1** was tested by measuring the fluorescent response over 30 min under constant excitation. Fig. S6.†

showed the time-course fluorescence intensity of **1** (60 μM) in aqueous solution at pH 6.00 and 7.00 at 37 °C. The fluorescence intensity at 516 and 559 nm remained stable over the time range tested. Furthermore, the fluorescence ratio ($I_{516\ nm}/I_{559\ nm}$) exhibited little variation when the temperature changed from 20 to 40 °C (Fig. S7. †). These experiments indicated that **1** could steadily respond to pH values without interference from photobleaching and variation in temperature.

Considering that a number of salicylaldehyde Schiff base derivatives can chelate di- or tri-valent metal ions in solution,[18] the selectivity of **1** to H^+ over metal ions was investigated by competition experiments. The fluorescence intensity of **1** displayed moderate variation in the absence or presence of an excess of Li^+, K^+, Zn^{2+}, Mg^{2+}, Ca^{2+}, Fe^{3+}, Cu^{2+}, Mn^{2+} and Cd^{2+} ions at pH 5.98 and pH 6.80. However, as shown in Fig. 5, no significant changes in the intensity ratio ($I_{516\ nm}$ / $I_{559\ nm}$) were observed, which indicated that the interference from these metal ions on ratiometric fluorescence pH measurements were negligible.

With satisfied selectivity over metal ions, we realized **1** could be utilized as an excellent ratiometric fluorescent pH indicator for real water samples (Table S1†).

Detection of H^+ in live cells by confocal microscopy

To further demonstrate the application of the probe, we used **1** for fluorescence imaging of pH fluctuations in live cells. In this study, HepG2 cells were incubated with **1** (60 μM) and then with nigericin (5 μg mL^{-1}) to equilibrate the intracellular and extracellular pH, which is a standard approach that has previously been used to calibrate other pH measurements *in vitro*.[3c,19] As shown in Fig. 6 (a–f), **1** was well-distributed within live cells (bright-field transmission image confirmed the viability of the cells,[2d,20] see Fig. 6 (j)), indicating excellent membrane permeability. The dye-loaded cells exhibited weak fluorescence in both channel I (490–535 nm) and channel II (540–585 nm) in PBS at pH 5.00; whereas the fluorescence brightness of channel I was obviously enhanced as the pH was increased. The ratiometric fluorescence images were shown in Fig. 6 (g–i), which demonstrated that **1** could readily reveal near-neutral pH variations in HepG2 cells by a ratiometric response. The mean fluorescent intensity (MFI) and fluorescence ratio of channel I and channel II were acquired using commercial software and are displayed in Fig. 6 (k) (fluorescence images of dye-loaded cells in PBS at pH

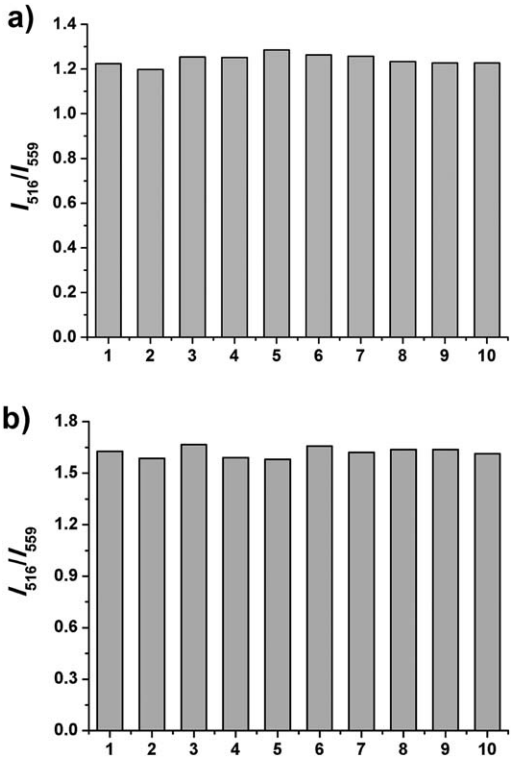

Fig. 5 Ratio of fluorescence intensity at 516 nm and 559 nm of **1** (60 μM) in the absence or presence of 300 μM Zn^{2+}, Fe^{3+}, Cu^{2+}, Mn^{2+}, Cd^{2+}, 5 mM Mg^{2+}, Ca^{2+}, and 10 mM Li^+, K^+ ions in phosphate buffer solution at pH 5.98 (a) and 6.80 (b). 1: H^+, 2: Li^+, 3: K^+, 4: Zn^{2+}, 5: Mg^{2+}, 6: Ca^{2+}, 7: Fe^{3+}, 8: Cu^{2+}, 9: Mn^{2+}, 10: Cd^{2+}. Excitation was performed at 353 nm.

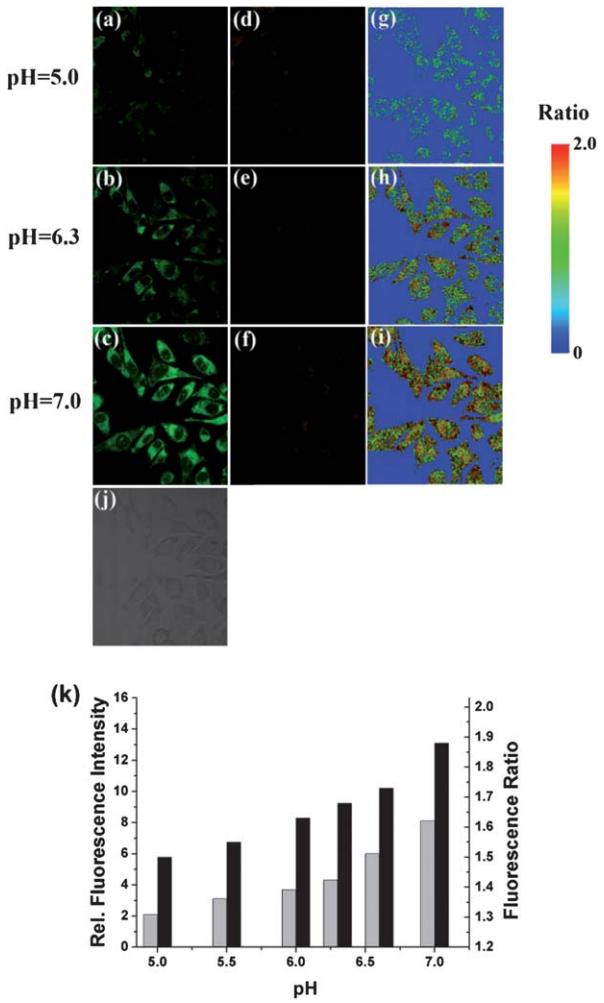

Fig. 6 Confocal fluorescence images of H^+ in HepG2 cells after incubation with **1** (60 μM) and nigericin at 37 °C (λ_{ex} = 405 nm). Left: collected at channel I (490–535 nm) at pH 5.00 (a), 6.30 (b), and 7.00 (c); middle: collected at channel II (540–585 nm) at pH 5.00 (d), 6.30 (e), and 7.00 (f); and right (g–i): ratiometric fluorescence images generated from channel I and channel II; (j) bright-field transmission image of (c). (k) Data of mean fluorescent intensity (MFI) (gray bar) and fluorescence ratio of channel I and channel II (black bar) at various pH of 5.00, 5.50, 6.00, 6.30, 6.60, 7.00.

5.50, 6.00, and 6.60 are shown in Fig. S8.†). These results have established that probe **1** is a good candidate for monitoring pH fluctuations in live cells.

Conclusion

In conclusion, a ratiometric fluorescent pH indicator 4-carboxylaniline-5-chlorosalicylaldehyde Schiff base (**1**) was synthesized *via* a facile method and used to monitor pH fluctuations both in aqueous solution and in live cells. Compound **1** displayed strong aggregation-induced emission enhancement (AIEE) fluorescence in its aggregate/solid state, resulting from the restriction of free intramolecular rotation of a C–N single bond and its non-planar configuration in such a state. A significant fluorescence color change from orange to green with intensity ratio ($I_{516\ nm}/I_{559\ nm}$) enhancement was observed over a pH range from 5.0 to 7.0. The new probe displays several advantageous properties including ratiometric fluorescence over a near-neutral pH response range, high tolerance to metal ions, and excellent stability, all of which were favourable for intracellular pH imaging. Application of **1** for pH imaging in live HepG2 cells was successfully achieved, proving that **1** can reveal intracellular pH fluctuations *via* a ratiometric response.

Experimental section

Chemicals

Analytical grade absolute ethanol and deionized water (distilled) were used throughout the experiment as solvents. All materials for synthesis were purchased from Alfa Aesar Co. and used without further purification. Nigericin (sodium salt) was bought from Fermentek Ltd. HepG2 cells were kindly provided by Prof. J.M. Lin's research group at Tsinghua University. Solutions of metal ions were prepared from the corresponding nitrate salts (analytical grade), except for KCl and $MnCl_2$. Phosphate buffer solutions (50 mM) at various pH values were prepared under adjustment by a pH meter using different ratios of phosphoric acid, sodium dihydrogen phosphate, disodium hydrogen phosphate and sodium hydroxide.

Instruments

Absorption spectra were measured on a JASCO V-550 UV-vis spectrophotometer. Fluorescence spectra measurements were performed on a JASCO FP-6500 spectrofluorimeter equipped with a xenon discharge lamp, using 1 cm quartz cells. All pH measurements were made with a METTLER TOLEDO 320 pH meter (Shanghai, China). NMR spectra were recorded using a JOEL JNM-ECA300 spectrometer operated at 300 MHz. ESI-MS spectra were obtained on a HP 1100 LC–MS spectrometer. X-ray crystal data collection was controlled by XSCANS program. Computations were constructed using the SHELXTL NT ver. 5.10 program package on an IBM PC 586 computer. Dynamic light scattering (DLS) experiments were conducted using a ZETA3000HS (3 nm–3 μm) light scattering instrument. Scanning electron microscopy (SEM) observations were performed on a KYKY-2000 instrument. Fluorescent images were taken using a LMS 710 confocal laser scanning microscope (Carl Zeiss Co., Ltd.) with an objective lens (×40). Unless otherwise mentioned, all of the measurements were operated at room temperature and repeated at least once.

Synthesis of compound 1

In a 50 mL flask, 3 mmol of 5-chlorosalicylaldehyde and 3 mmol of 4-carboxyaniline were dissolved in 25 mL of ethanol, and stirred at room temperature overnight. The resulting precipitate was filtered and washed three times with 15 mL of cold ethanol. After drying, **1** was obtained as an orange solid in a 62% yield (Scheme S1 †). ^{1}H NMR (300 MHz, DMSO-d_6, 25 °C, TMS) δ (ppm) = 7.02 (d, J_1 = 8.6 Hz, J_2 = 2.8 Hz, H), 7.46 (d, J = 8.2 Hz, H), 7.48 (d, J = 8.6 Hz, 2H), 7.78 (d, J = 2.8 Hz, H), 8.01 (d, J = 8.2 Hz, 2H), 8.96 (s, H); ^{13}C NMR (300 MHz, DMSO-d_6, 25 °C, TMS) δ (ppm) = 119.3, 121.2, 122.1, 123.3, 129.6, 131.3, 131.4, 133.8, 152.6, 159.4, 163.6, 167.4; ESI mass spectrometry: m/z 274.2 ([M − H]$^-$); M$^-$ calcd 274.0; elemental analysis calcd (%) for $C_{14}H_{10}ClNO_3$: C 61.09, H 3.67, Cl 12.72, N 5.09, O 17.43; found: C 60.91, H 3.69, Cl 12.81, N 5.14, O 17.45.

Crystal structure determination of compound 1

Crystal data. $C_{14}H_{10}ClNO_3$, M = 275.68, monoclinic, a = 6.177(2) Å, b = 7.001(3) Å, c = 28.415(10) Å, α = 90.00°, β = 94.40(3)°, γ = 90.00°, V = 1225.1(8) Å3, T = 295 ± 2 K, space group C_2/m (No. 12), Z = 4, 1863 reflections measured, 1244 unique reflections (R_{int} = 0.0912) which were used in all calculations. R_1 = 0.0808, wR_2 = 0.1405, CCDC: 780526.†

Spectral measurements

A stock solution of **1** (3 mM) was prepared in ethanol. Absorption and fluorescence measurements were performed by addition of a proper amount of stock solutions to buffered water or buffered water/ethanol of different pH and ethanol fractions (totally 3 mL) in a 1 cm quartz cell. After mixing, the solutions were allowed to stand at ambient conditions for 5 min, and then absorption or fluorescence spectra were recorded.

Determination of pK_a from absorption titration

For determination of pK_a, 10 μM of **1** was prepared in aqueous solution at various pH levels for absorption titration. At this concentration, **1** was in the "solution" state with structured absorption spectra. The proton dissociation constants pK_{a1} and pK_{a2} of **1** were calculated from the results of a nonlinear regression of the absorbance at 290 nm and 390 nm, as previously described.[4b, 21]

pH-dependent intracellular fluorescence imaging

Human hepatocellular liver carcinoma cell line (HepG2 cells) were incubated in Dulbecco's modified Eagle's medium (DMEM) supplemented with 10% fetal bovine serum (FBS), penicillin (100 units mL^{-1}), and streptomycin (100 μg mL^{-1}). Cultures were maintained at 37 °C under a humidified atmosphere containing 5% CO_2. About 1.0 × 10^5 HepG2 cells in growth medium (2 mL) were seeded on a 35 mm-diameter round glass petri dish and incubated overnight at 37 °C under 5% CO_2. The medium was then removed. The cells were incubated with

a solution of **1** (60 μM) in medium (2 mL) for 10 min under the same conditions. After that, the medium was removed and the cells were treated with nigericin (5 μg mL^{-1}) in PBS (2 mL) for further 10 min. Before imaging, the dye loaded cells were rinsed three times and incubated with PBS buffer (50 mM) at various pH values (pH = 5.0, 5.5, 6.0, 6.3, 6.6, 7.0) for 10 min, respectively.

Cells were imaged with a LMS 710 confocal laser scanning microscope equipped with a Chamlide TC system (Live Cell Instrument, Inc.). The excitation wavelength was 405 nm. Emission signals from 490–535 nm and 540–585 nm were collected and denoted channel I and channel II, respectively, and images were analysed using Image-Pro Plus software. The intracellular fluorescence intensities and fluorescence ratio of channel I and channel II were also determined, using a total of 10 cells at each pH tested.

Calculation of quantum yield

Quantum yields were calculated using quinine sulfate in 0.1 M H_2SO_4 (excitation at 366 nm) as a standard ($\Phi = 0.55$) for solution phase samples. For solid phase samples, an integral sphere was applied with $BaSO_4$ white plates as a standard ($\Phi = 1.0$).[11]

Acknowledgements

This work was financially supported by the National Natural Science Foundation of China (NSFC, Nos. 20875054 and 90813014). The authors thank Dr H. F. Li and Prof. J. M. Lin for kindly providing us the cells. We also thank Prof. R. J. Wang for the analysis of X-ray crystal data.

References

1 (*a*) R. A. Gottlieb and A. Dosanjh, *Proc. Natl. Acad. Sci. U. S. A.*, 1996, **93**, 3587; (*b*) K. Xu and A. M. Klibanov, *J. Am. Chem. Soc.*, 1996, **118**, 9815; (*c*) R. M. Zaguilln and R. J. Gillies, *Cell. Physiol. Biochem.*, 1996, **6**, 169; (*d*) B. Tang, F. B. Yu, P. Li, L. L. Tong, X. Duan, T. Xie and X. Wang, *J. Am. Chem. Soc.*, 2009, **131**, 3016.

2 (*a*) M. Stubbs, P. M. J. McSheehy, J. R. Griffiths and C. L. Bashford, *Mol. Med. Today*, 2000, **6**, 15; (*b*) J. Srivastava, D. L. Barber and M. P. Jacobson, *Physiology*, 2007, **22**, 30; (*c*) J. Y. Han and K. Burgess, *Chem. Rev.*, 2010, **5**, 2709.

3 (*a*) Y. Xiang and A. J. Tong, *Chem. Lett.*, 2005, **34**, 926; (*b*) X. Y. Peng, J. J. Du, J. L. Fan, J. Y. Wang, Y. K. Wu, J. Z. Zhao, S. G. Sun and T. Xu, *J. Am. Chem. Soc.*, 2007, **129**, 1500; (*c*) J. Y. Han, A. Loudet, R. Barhoumi, R. C. Burghardt and K. Burgess, *J. Am. Chem. Soc.*, 2009, **131**, 1642; (*d*) L. Xue, C. Liu and H. Jiang, *Chem. Commun.*, 2009, 1061; (*e*) Z. X. Han, X. B. Zhang, Z. Li, Y. J. Gong, X. Y. Wu, Z. Jin, C. M. He, L. X. Jian, J. Zhang, G. L. Shen and R. Q. Yu, *Anal. Chem.*, 2010, **82**, 3108.

4 (*a*) N. N. Ratchford, S. Bangsaruntip, X. M. Sun, K. Welsher and H. J. Dai, *J. Am. Chem. Soc.*, 2007, **129**, 2448; (*b*) S. Yao, K. J. S. Hales and K. D. Belfield, *Org. Lett.*, 2007, **9**, 5645; (*c*) M. T. Chen, L. M. Gomez, F. N. Ishikawa, P. T. Vernier, C. Zhou and M. A. Gundersen, *Nanotechnology*, 2009, **20**, 295101; (*d*) X. J. Jiang, P. C. Lo, S. L. Yeung, W. P. Fong and D. K. P. Ng, *Chem. Commun.*, 2010, **46**, 3188.

5 (*a*) Y. N. Hong, J. W. Y. Lama and B. Z. Tang, *Chem. Commun.*, 2009, 4332; (*b*) M. Wang, X. G. Gu, G. X. Zhang, D. Q. Zhang and D. B. Zhu, *Anal. Chem.*, 2009, **81**, 4444; (*c*) Q. Chen, N. Bian, C. Cao, X. L. Qiu, A. D. Qi and B. H. Han, *Chem. Commun.*, 2010, **46**, 4067; (*d*) Y. Liu, Y. Yu, J. W. Y. Lam, Y. N. Hong, M. Faisal, W. Z. Yuan and B. Z. Tang, *Chem.–Eur. J.*, 2010, **16**, 8433; (*e*) Y. Liu, C. M. Deng, L. Tang, A. J. Qin, R. R. Hu, J. Z. Sun and B. Z. Tang, *J. Am. Chem. Soc.*, 2011, **133**, 660; (*f*) J. P. Xu, Z. G. Song, Y. Fang, J. Mei, L. Jia, A. J. Qin, J. Z. Sun, J. Ji and B. Z. Tang, *Analyst*, 2010, **135**, 3002.

6 (*a*) H. Y. Li, Z. G. Chi, B. J. Xu, X. Q. Zhang, X. F. Li, S. W. Liu, Y. Zhang and J. R. Xu, *J. Mater. Chem.*, 2011, **21**, 3760; (*b*) M. Wang, G. X. Zhang, D. Q. Zhang, D. B. Zhu and B. Z. Tang, *J. Mater. Chem.*, 2010, **20**, 1858; (*c*) A. Dreuw, J. Plöner, L. Lorenz, J. Wachtveitl, J. E. Djanhan, J. Brüning, T. Metz, M. Bolte and M. U. Schmidt, *Angew. Chem., Int. Ed.*, 2005, **44**, 7783.

7 J. Luo, Z. Xie, J. W. Y. Lam, L. Cheng, H. Chen, C. Qiu, H. S. Kwok, X. Zhan, Y. Q. Liu, D. B. Zhu and B. Z. Tang, *Chem. Commun.*, 2001, 1740.

8 (*a*) L. H. Chan, R. H. Lee, C. F. Hsieh, H. C. Yeh and C. T. Chen, *J. Am. Chem. Soc.*, 2002, **124**, 6469; (*b*) S. J. Lim, B. K. An, S. D. Jung, M. A. Chung and S. Y. Park, *Angew. Chem., Int. Ed.*, 2004, **46**, 6346; (*c*) Z. J. Zhao, S. M. Chen, X. Y. Shen, F. S. Mahtab, Y. Yu, P. Lu, J. W. Y. Lam, H. S. Kwoka and B. Z. Tang, *Chem. Commun.*, 2010, **46**, 686; (*d*) X. Feng, B. Tong, J. B. Shen, J. B. Shi, T. Y. Han, L. Chen, J. G. Zhi, P. Lu, Y. G. Ma and Y. P. Dong, *J. Phys. Chem. B*, 2010, **114**, 16731.

9 (*a*) Y. Liu, Y. Tang, N. N. Barashkov, I. S. Irgibaeva, J. W. Y. Lam, R. Hu, D. Birimzhanova, Y. Yu and B. Z. Tang, *J. Am. Chem. Soc.*, 2010, **132**, 13951; (*b*) J. Wang, J. Mei, W. Z. Yuan, P. Lu, A. J. Qin, J. Z. Sun, Y. G. Ma and B. Z. Tang, *J. Mater. Chem.*, 2011, **21**, 4056; (*c*) Z. J. Ning, Z. Chen, Q. Zhang, Y. L. Yan, S. X. Qian, Y. Cao and H. Tian, *Adv. Funct. Mater.*, 2007, **17**, 3799.

10 (*a*) C. J. Bhongale and C. S. Hsu, *Angew. Chem., Int. Ed.*, 2006, **45**, 1404; (*b*) K. Kokado and Y. Chujo, *J. Org. Chem.*, 2011, **76**, 316; (*c*) J. Chen, H. Peng, C. C. W. Law, Y. Dong, J. W. Y. Lam, I. D. Williams and B. Z. Tang, *Macromolecules*, 2003, **36**, 4319.

11 W. X. Tang, Y. Xiang and A. J. Tong, *J. Org. Chem.*, 2009, **74**, 2163.

12 (*a*) Y. Dong, J. W. Y. Lam, A. Qin, Z. Li, J. Liu, J. Sun, Y. Dong and B. Z. Tang, *Chem. Phys. Lett.*, 2007, **446**, 124; (*b*) Z. Li, Y. Q. Dong, J. W. Y. Lam, J. X. Sun, A. J. Qin, M. Haeussler, Y. P. Dong, H. H. Y. Sung, I. D. Williams, H. S. Kwok and B. Z. Tang, *Adv. Funct. Mater.*, 2009, **19**, 905.

13 X. T. Chen, Y. Xiang, N. Li, P. S. Song and A. J. Tong, *Analyst*, 2010, **135**, 1098.

14 (*a*) D. E. Janzen, M. W. Burand, P. C. Ewbank, T. M. Pappenfus, H. Higuchi, D. A. Filho, V. G. Young, J. L. Brédas and K. R. Mann, *J. Am. Chem. Soc.*, 2004, **126**, 15295; (*b*) Z. J. Ning, Y. C. Zhou, Q. Zhang, D. G. Ma, J. J. Zhang and H. Tian, *J. Photochem. Photobiol., A*, 2007, **192**, 8; (*c*) Y. Q. Dong, J. W. Y. Lam, A. J. Qin, Z. Li, J. Z. Sun, H. H.-Y. Sung, I. D. Williamsa and B. Z. Tang, *Chem. Commun.*, 2007, 40.

15 (*a*) B. Z. Tang, Y. Geng, J. W. Y. Lam, B. Li, X. Jing, X. Wang, F. Wang, A. Pakhomov and X. X. Zhang, *Chem. Mater.*, 1999, **11**, 1581; (*b*) S. Kamino, Y. Horio, S. Komeda, K. Minoura, H. Ichikawa, J. Horigome, A. Tatsumi, S. Kaji, T. Yamaguchi, Y. Usami, S. Hirota, S. Enomoto and Y. Fujita, *Chem. Commun.*, 2010, **46**, 9013.

16 (*a*) D. Oelkrug, A. Tompert, J. Gierschner, H. Egelhaaf, M. Hanack, M. Hohloch and E. Steinhuber, *J. Phys. Chem. B*, 1998, **102**, 1902; (*b*) B. K. An, S. K. Kwon, S. D. Jung and S. Y. Park, *J. Am. Chem. Soc.*, 2002, **124**, 14410; (*c*) Y. F. Zhao, H. Z. Gao, Y. Fan, T. L. Zhou, Z. M. Su, Y. Liu and Y. Wang, *Adv. Mater.*, 2009, **21**, 3165; (*d*) Y. Qian, S. Y. Li, G. Q. Zhang, Q. Wang, S. Q. Wang, H. J. Xu, C. Z. Li, Y. Li and G. Q. Yang, *J. Phys. Chem. B*, 2007, **111**, 5861.

17 (*a*) A. Pross, L. Radom and R. Taft, *J. Org. Chem.*, 1980, **45**, 818; (*b*) Z. Rappoport, *The Chemistry of Phenols*, John Wiley & Sons, Chichester, 2003; (*c*) Y. Fan, Y. M. Zhu, F. R. Dai, L. Y. Zhang and Z. N. Chen, *Dalton Trans.*, 2007, 3885; (*d*) Z. Q. Guo, P. Zhao, W. H. Zhu, X. M. Huang, Y. S. Xie and H. Tian, *J. Phys. Chem. C*, 2008, **112**, 7047.

18 (*a*) L. K. Charkoudian, D. M. Pham and K. J. Franz, *J. Am. Chem. Soc.*, 2006, **128**, 12424; (*b*) N. Li, Y. Xiang and A. J. Tong, *Chem. Commun.*, 2010, **46**, 3363.

19 (*a*) J. A. Thomas, R. N. Buchsbaum, A. Zimniak and E. Racker, *Biochemistry*, 1979, **18**, 2210; (*b*) J. Llopis, J. M. McCaffery, A. Miyawaki, M. G. Farquhar and R. Y. Tsien, *Proc. Natl. Acad. Sci. U. S. A.*, 1998, **95**, 6803.

20 W. S. Zhang, B. Tang, X. Liu, Y. Y. Liu, K. H. Xu, J. P. Ma, L. L. Tong and G. W. Yang, *Analyst*, 2009, **134**, 367.

21 E. J. Billo, *Excel for Chemists, in A Comprehensive Guide*, Wiley-VCH, New York, 1997, pp. 303.